

Alexandre Carbonnel^a, Hugo Pérez^a, María Ignacia Lucares^a, Daniel Escobar^a, María Paz Jiménez^a, Dayana Gavilanes^b,

^a Environmental Architectural Materials Laboratory (LEMAA), School of Architecture, University of Santiago, Chile

^b Polymers Laboratory, Faculty of Chemistry and Biology, University of Santiago, Chile

alexandre.carbonnel@usach.cl

hugo.perez.h@usach.cl

maria.lucares@usach.cl

daniel.escobar@usach.cl

pazjimenezvilla@gmail.com

dgavilanes.ruiz@gmail.com

Abstract. Consideration of plastic waste as a secondary raw material obtainable by means of upcycling presents fresh possibilities in the search for new construction and architectural materials. This paper demonstrates the possibility of recycling thermoplastic polyethylene terephthalate (PET) and the potential for enhancement of its properties through the incorporation of nanoparticles. The design of materials by means of managed complexity involving processes of *materialisation* and *configuration* is explored by processing film from recycled plastic and their subsequent assessment as a possible semi-finished product with photocatalytic potential.

Keywords: Upcycling; Photocatalysis; Materials design; Plastic recycling; Nanotechnology.

Introduction

Some directives (CE, 2015) propose that waste should be considered as a secondary raw material with potential for reintroduction into productive cycles. Considering the risks posed by plastic to health and ecosystems (CE, 2013), there is an urgent need to boost recycling.

In 2016, 242 Mt of plastic waste were produced worldwide, accounting for 12% of municipal solid waste (WBG, 2018). In 2015, the European Union recycled 25% of its plastic waste (CE, 2015), a figure far greater than that achieved by Chile, which only reached 8.5% (ASIPLA, 2019).

In light of this, the present study adopts an exploratory approach to the problem of plastic waste, and views the latter, following a process of upcycling, as a secondary raw material for the design of construction materials.

Some studies refer to upcycling in the development of components for construction or architecture (Rose and Stegemann, 2018; Baiani and Altamura, 2018). Baiani & Altamura (2018) focus on upcycling in the experimental design and development of technical solutions for concrete elements, such as paving blocks and stones, incorporating recycled additives in a process referred to as “superuse”. This approach considers upcycling to be an evolution of recycling that yields an improvement in the value or functionality of the original material (Rose and Stegemann, 2018).

The study, therefore, views upcycling as *managed complexity*, and adopts the materials design objectives posed by Ezio Manzini (1992), defining this complexity by exploring the mechanical recycling process of polyethylene terephthalate (PET), as well as the potential environmental function of degrading atmospheric contaminant gases through the addition of a titanium dioxide (TiO₂) semiconductor that would generate a photocatalytic reaction (Fig. 1).

Design hypothesis: a new and improved material based on recycled PET and TiO₂

The design hypothesis rests on two questions. What is the potential of PET waste recycling for the development of

materials? Can PET waste be repurposed to develop a new material with photocatalytic potential through the incorporation of nanoparticles?

In order to answer these questions, the present study employs a process of three *materialisations* to produce a set of materials: (1) titanium dioxide (TiO₂) nanoparticles, (2) recycled PET, and (3) recycled PET mixed with TiO₂. This is followed by the configuration of three series of plastic film, each providing seven samples for study and testing.

Materialisations and *configurations* are each conditional on two developmental frameworks (DF). The former, DF1, encompasses technology in the form of machines and instruments (see Figure 2), while the latter, DF2, covers the regulatory provisions applicable to polymer-based construction materials.

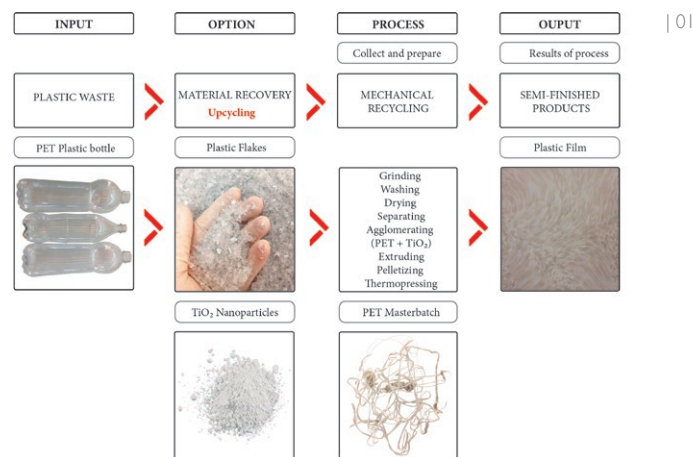
DF1 included the Labtech LP20-B press, which enabled us to create films with maximum size 150x150 mm between its stainless-steel plates. This was the first step in the *configuration* process. DF2 covered national and international standards and, beginning with the validation of variables, sample dimensions and testing methods, allowed us to speculate as to the use of the *semi-finished product* as a building material, adjusting the thickness of the film as a second step in the *configuration* process.

The “Chilean standard – construction – plastic tiles – testing methods (NCh 873:1999)” establishes two thickness test ranges from 2.4 to 3.2 mm and from 1.4 to 1.6 mm. The standard for “Determination of the behaviour of self-supporting plastics in response to a flame (NCh 2121/1)” specifies a test thickness of 3–12 mm.

In accordance with these standards and considering the film as a possible semi-finished product – tiles or cladding – we decided upon a minimum thickness of 3 mm for their *configuration*.

The film *configuration* adjustments were as follows: Series A, based on pressed PET flakes (PETr-t); Series B based on extruded and pressed PET flakes (PETr-e); and Series C (the new material) consisting of PET flakes extruded with TiO₂ nanoparticles and pressed (PETr-e-TiO₂).

Finally, in order to answer the questions posed by the design hypothesis, four sets of measurements and observations (MO) were made of the resulting film. MO1 was a qualitative evaluation of the three series, which resulted in the selection – based on their physical characteristics – of the best Series B and C films with which we would then move on to the subsequent MOs. MO2 consisted of a Differential Scanning Calorimetry (DSC) conducted on a sample of the films selected at MO1 in order to observe the thermal properties of the polymer and any possible variations following the heat treatments involved by extrusion



and pressing. MO3 consisted of Transmission Electron Microscopy (TEM) that allowed us to establish the presence of nanoparticles in the polymer. Finally, MO4 was Scanning Electron Microscopy (SEM), which allowed us to visualise and quantify the presence of TiO_2 nanoparticles on the surface and within the microstructural morphology of the new material, PETr-e- TiO_2 .

Materialisations and configurations: exploration methods

The procedure began with the collection of plastic bottles (input) and their classification (plastic waste), and culminated in the development of a semi-finished product with improved properties as a result of upcycling.

Materialisation (1): TiO_2 nanoparticles synthesis

Synthesis of spherical TiO_2 was achieved by means of the sol-gel method, using titanium isopropoxide ($\text{Ti}[\text{OCH}(\text{CH}_3)_2]$) as a precursor (Aldrich, 97%). Two solutions were prepared at room temperature. To prepare the first solution, 5 mL of titanium isopropoxide (IV), measured in a nitrogen atmosphere, were added to 15 mL of isopropanol (Equilab, 99%). To prepare the second solution, 3M nitric acid (HNO_3) (Aldrich, 90%) was added to 250 mL of distilled water, bringing the solution to a pH level of 2. Once the two solutions had been prepared, the second was placed in a silicon bath above a heating plate set to 60°C and stirred while the first solution was added dropwise. The resulting mixture was stirred at 60°C for 20 hours, then placed on a heating plate set to 80°C . The solvent evaporated to leave yellow crystals, which were then washed with ethanol and vacuum filtered. Finally, the $n \text{TiO}_2$ were calcinated in a muffle furnace at 200°C for 4 hours, after which they were ready for incorporation into the PET.

Materialisation (2) and (3): production of recycled PET mixed with TiO_2 nanoparticles

The molecular structure of PET may be amorphous or semi-crystalline, with maximum 45% crystallinity. The amorphous portion gives the material its elastic properties, while the crystallinity – the result of a specific molecular order – provides resistance to mechanical force. The glass transition temperature (T_g) is reached when the polymer chains acquire a degree of molecular movement, giving the material elasticity and causing

it to pass from a glassy state to a rubbery one (transition). The melting temperature (T_m) is the temperature at which crystals form (transformation) and the polymer passes from a solid to a viscous liquid state, acquiring fluidity and losing its mechanical properties.

The mixing of recycled PET (PETr) with TiO_2 involved a six-step process (Fig. 2). Used transparent PET bottles were collected (1), manually washed (2) and ground into flakes (3). Several loads of 1000 g of PET were processed in the grinder (equipped with a 4 mm screen) for 10 minutes each. This produced a secondary raw material in the form of flakes (ISO 15270; 2018).

The mixture of PETr and TiO_2 was created by extrusion. The process uses a *configuration* of heat, pressure and rotation to combine the PETr with TiO_2 , extruding a new polymeric material in a filament known as Masterbatch. This is finally cooled in water and pelletised to form the new secondary raw material PETr-e- TiO_2 .

Three sequential extrusions were made. Firstly, 400 g of PETr were extruded as a cleaning routine in order to avoid contamination of the sample. Secondly, 900 g of PETr were extruded to produce a pelletised Masterbatch as a secondary raw material for the creation of film for comparison. Finally, 690 g of PETr were combined with 60 g of TiO_2 nanoparticles (8% of the sample) in the extruder's hopper.

Configuration: pressing and production of the three series of film

The configuration process, based on DF1 and DF2, determined the testing of film with dimensions of $150 \times 150 \times 3$ mm. Series A: flakes (PETr-t); Series B: extrusion (PETr-e); Series C: extrusion of mixture with TiO_2 nanoparticles (PETr-e- TiO_2). Configurations were achieved by adjusting the pressing variables (Fig.3).

Measurements and Observations of the film: development of the 4 MOs.

MO1: Qualitative analysis was conducted of five physical characteristics. These were visually assessed and entered into a matrix using a scale of 0 to 5, where a lower score corresponded to better film performance. The aim was to identify the best film samples to take forward for testing, based on the criteria of fragility, presence of bubbles, calcination, presence of fissures, and heterogeneity.

MO2: the glass transition temperature (T_g), melting temperature (T_m) and enthalpy of fusion (ΔH) of the second and third series as

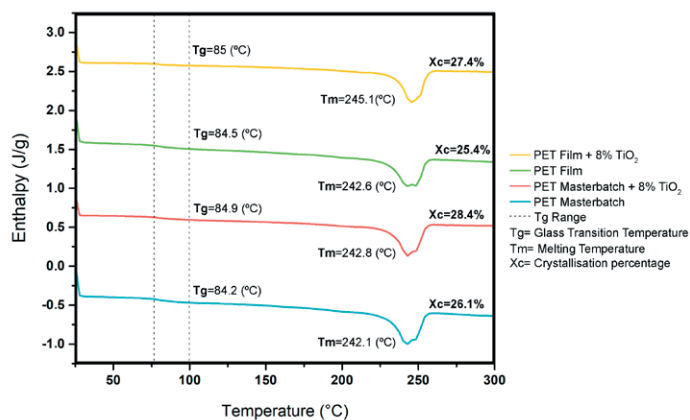
TYPE OF MATERIALISATION	STAGES OF CONFIGURATION PROCESS									
SYNTHESIS OF TITANIUM DIOXIDE TiO ₂ NANOPARTICLES (No. 1)	A	B	C	D	E	F				
		Preparation of solution 1 (titanium isopropoxide added to isopropanol)	Preparation of solution 2 (nitric acid added to distilled water)	Solution 1 added dropwise to solution 2	Evaporation of solvent	Vacuum Filtration	Calcination			
PROCESS ASSISTED BY MACHINE					Boeco R-430 Vacuum/Pressure Pump	Thermo Scientific Lindberg Blue Muffle Furnace				
PROCESS ASSISTED BY INSTRUMENTS	Round-bottom flask 100 mL	Erlenmeyer flask 500 mL	Heating Plate Thermometer	Heating Plate Beaker Thermometer		Mortar				
MATERIALS	MEASUREMENT									
ISOPROPANOL (mL)	15									
TITANIUM ISOPROPOXIDE (mL)	5									
ETHANOL (mL)					50					
NITRIC ACID [M]		3								
pH OF THE SOLUTION		2								
DISTILLED WATER (L)		0,25								
TEMPERATURE (°C)			60	80		200				
TIME (min)			20	24		4				
RECYCLING PROCESS OF POLYETHYLENE TEREPHTHALATE (PET) MIXED WITH TITANIUM DIOXIDE NANOPARTICLES TiO ₂ (No. 2 & 3)	1	2	3	4	5	6	6F	7	8	8F
	STORAGE OF BOTTLES	WASHING OF BOTTLES	GRINDING /GENERATION OF PET FLAKES	WASHING OF PET FLAKES	DRYING OF PET FLAKES	EXTRUSION OF PET FLAKES	EXTRUSION OF PET FLAKES WITH NANO-PARTICLES	PETr-t FLAKE PRESSING: SERIES A (7 films)	PETr-e MASTER-BATCH PRESSING: SERIES B (7 films)	PETr-e-TiO ₂ MASTER-BATCH PRESSING: SERIES C (7 films)
MANUAL PROCESS	35 bottles (size 3 L)	35 bottles (size 3 L)					Mixing PETr-e + TiO ₂			
PROCESS ASSISTED BY MACHINE			Thera A200-E Grinder/ 4 mm strainer		Elos "Heat" HO55F Heating Oven	Labtech 20-40 Twin Screw Extruder	Labtech 20-40 Twin Screw Extruder	Labtech LP20-B Press	Labtech LP20-B Press	Labtech LP20-B Press
PROCESS ASSISTED BY INSTRUMENTS	Storage tray 120 L			Sifter 250 microns Steel spatula Brush No. 8-14	Drying tray Aluminium foil	Beaker Steel spatula Brush No. 8-14	Beaker Steel spatula Brush No. 8-14	Kern PFB 200-3 Balance Steel matrix Teflon (3 mm) Beaker Brush No. 8-14	Kern PFB 200-3 Balance Steel matrix Teflon (3 mm) Beaker Brush No. 8-14	Kern PFB 200-3 Balance Steel matrix Teflon (3 mm) Beaker Brush No. 8-14
MATERIALS	MEASUREMENT									
WATER / DISTILLED WATER (L)		105		3						
PET MATERIAL WEIGHT (g)			2040	2040		900	690	568	621	630
TiO ₂ MATERIAL WEIGHT (g)							60			60
PRESSURE (bar)						45	47,5	70 - 90	80 - 90	55 - 80
TEMPERATURE (°C)					60 - 80	255	255	255 - 260	260	260
TIME (min)		105	34			40	72	10 - 24	17 - 24	17

The combined scores for each characteristic provided the final value for each film. The best performance was achieved by films SSA2 and SSA6 (Series A), SSB2 and SSB3 (Series B), and SSC2, SSC3 and SSC6 (Series C)

both Masterbatch and film were measured using DSC (Mettler-Toledo DSC 1 STARe). The samples were heated from 25°C to 300°C at a rate of 10°C/min and then cooled to 25°C at the same rate. The readings were taken from the second heating curve in order to eliminate any thermal history. The percentage of crystallinity was calculated using the enthalpy of fusion of an ideal PET sample with 100% crystallinity (Blaine, 2002).

MO3: the morphology of the TiO₂ nanoparticles and their dispersion in film was analysed using TEM (Philips Tecnai 12) operating at 20 kV. Samples were prepared for TEM by placing a drop of TiO₂ on a carbon-coated standard copper grid (400 mesh) and evaporating the solvent. Figure 6A shows the TEM images of nanoparticles obtained using the sol-gel process, with spherical morphology and a diameter of ~10 [nm]. Figure 6E shows the TEM images of the TiO₂ structure.

MO4: on a nanometre scale, SEM images 7A and 7D show that the nanoparticles are not visually detectable in the polymer. Images 7B and 7E, generated using X rays (Energy-Dispersive Spectroscopy,



EDS) show the presence of three principal chemical elements: oxygen (yellow), carbon (blue), and titanium (green). Finally, images 7C and 7F show the presence of titanium only, with the other elements omitted.

Reflection and conclusions based on the MOs.

MO1 provided evidence of the importance of adjustments made to film configuration.

Series A highlighted the relationship between pre-contact time (3.5-8 min), contact time (3-6 min), and pressure (70-90 bar). These variable adjustments from SSA1 to SSA5 yielded improvements in terms

Series	Sample	Series A: Thermopressing Flakes PETr-t							Series B: Thermopressing Masterbatch PETr-e							Series C: Thermopressing Masterbatch PETr-e-TiO ₂						
		Material weight (g)	Melting temperature (°C)	Pressure (bar)	Pre Contact (min)	Contact (min)	Cooling (min)	Material weight (g)	Melting temperature (°C)	Pressure (bar)	Pre Contact (min)	Contact (min)	Cooling (min)	Material weight (g)	Melting temperature (°C)	Pressure (bar)	Pre Contact (min)	Contact (min)	Cooling (min)	Cooling pressure (bar)		
SERIES A:	SSA1	90	255	70	3.5	3	3	90	260	90	8	6	10	90	260	80	8	6	3	55		
	SSA2	23	260	70	5	4	15	90	260	80	8	3	90	260	80	8	3	60				
	SSA3	90	260	90	7	4	5	90	260	80	8	6	3	90	260	80	8	3	60			
	SSA4	90	260	90	8	5	5	87	260	80	10	6	3	90	260	80	8	6	3	60		
	SSA5	95	255	90	8	6	10	87	260	80	8	6	3	90	260	80	8	6	60			
	SSA6	90	260	90	7.5	6	10	87	260	80	8	6	3	90	260	80	8	6	60			
	SSA7	90	260	90	7.5	6	5	90	260	80	8	6	3	90	260	80	8	6	60			
SERIES B:	SSB1	90	260	90	8	6	10	87	260	80	10	6	3	90	260	80	8	6	3			
	SSB2	90	260	80	8	6	3	87	260	80	8	6	3	90	260	80	8	6	3			
	SSB3	90	260	80	8	6	3	87	260	80	8	6	3	90	260	80	8	6	3			
	SSB4	87	260	80	10	6	3	87	260	80	10	6	3	90	260	80	8	6	3			
	SSB5	87	260	80	8	6	3	87	260	80	8	6	3	90	260	80	8	6	3			
	SSB6	87	260	80	8	6	3	87	260	80	8	6	3	90	260	80	8	6	3			
	SSB7	90	260	80	8	6	3	90	260	80	8	6	3	90	260	80	8	6	3			
SERIES C:	SSC1	90	260	80	8	6	3	90	260	80	8	6	3	90	260	80	8	6	3			
	SSC2	90	260	80	8	3	60	90	260	80	8	3	60	90	260	80	8	3	60			
	SSC3	90	260	80	8	6	3	90	260	80	8	6	3	90	260	80	8	6	3			
	SSC4	90	260	80	8	6	3	90	260	80	8	6	3	90	260	80	8	6	3			
	SSC5	90	260	80	8	6	3	90	260	80	8	6	3	90	260	80	8	6	3			
	SSC6	90	260	80	8	6	3	90	260	80	8	6	3	90	260	80	8	6	3			
	SSC7	90	260	80	8	6	3	90	260	80	8	6	3	90	260	80	8	6	3			

PROCESS	PHYSICAL CHARACTERISTICS	SERIES A							SERIES B							SERIES C						
		SSA1	SSA2	SSA3	SSA4	SSA5	SSA6	SSA7	SSB1	SSB2	SSB3	SSB4	SSB5	SSB6	SSB7	SSC1	SSC2	SSC3	SSC4	SSC5	SSC6	SSC7
Pressing	Fragility	3.7	2.5	2.5	2.7	3.5	2.3	2.7	4.5	3.2	2.8	4.3	3.3	4.2	3.2	2.8	2.8	3.0	3.7	2.8	4.5	
	Bubbles	4.7	1.2	1.0	1.7	2.5	1.7	1.5	1.0	1.2	1.7	1.2	1.3	5.0	12.0	2.0	1.8	1.7	1.8	2.3	1.8	3.0
	Calcination	3.3	2.7	3.5	2.5	2.8	3.3	4.5	2.2	1.8	2.7	2.5	2.2	2.7	1.7	2.0	1.3	1.5	1.2	1.3	1.7	1.3
	Fissures	2.0	2.3	1.2	1.8	1.3	1.2	1.3	5.0	1.2	1.2	5.0	5.0	1.2	5.0	2.0	1.0	1.0	1.7	2.2	1.0	5.0
	Heterogeneity	5.0	1.8	1.8	1.8	4.3	1.8	2.5	3.2	2.7	2.8	2.7	2.2	4.2	2.8	1.8	1.5	1.7	1.7	3.0	1.3	3.5
Sample Total		18.7	10.5	10.0	10.5	14.5	10.3	12.5	15.8	10.0	11.2	15.8	15.0	16.3	14.8	11.0	8.5	8.7	9.3	12.5	8.7	17.3
Sample Average		12.43							14.14							10.86						

06 | TEM: visualisation of the presence of TiO₂

A) TiO₂ nanoparticles. B), C) and D) Film made from PETr + TiO₂ nanoparticles, different scales. E) Film PETr + TiO₂, showing their anatase structure

07 | SEM: identification of TiO₂ nanoparticles

A) and D) Film surface and cross-section. B) and E) film surface and cross-section Oxygen (yellow), titanium (green) and carbon (blue). C) and F) titanium isolated on film surface and in cross-section

of reduced heterogeneity, fissures and bubbles (Fig. 3). From SSA3 onward, temperature was fixed at 260°C. This provided optimum melting, avoiding calcination.

Series B film presented greater fragility, possibly due to the heat treatment involved in extrusion. To correct this, pressure was adjusted to 80 bar and cooling time was reduced to 3 min from SSB2 onward in order to avoid excess fissures and crystallisation. From sample SSB3 onward, a number of problems became apparent, possibly attributable to the weight reduction to 87 g. At SSB7, therefore, weight was restored to 90 g.

Finally, the previous parameters were maintained for the entire Series C, with the only change being to 60 bar of pressure during the cooling phase. This adjustment reduced fragility and fissures in the samples.

This iterative process across the three series of *materialisation* produced improvements in film *configuration* thanks to the use of machines (DF1). Adjustments to pressure, pre-contact time and contact time had the most meaningful effects.

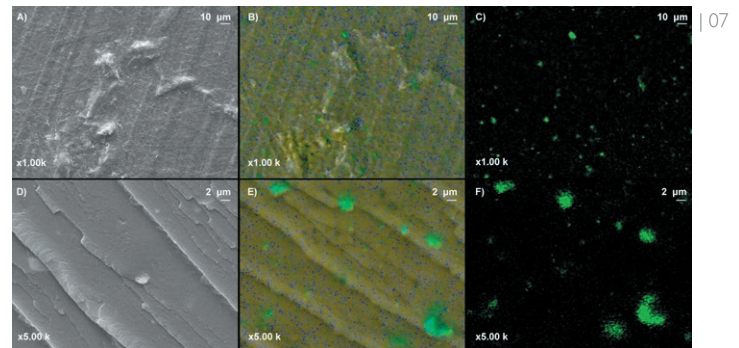
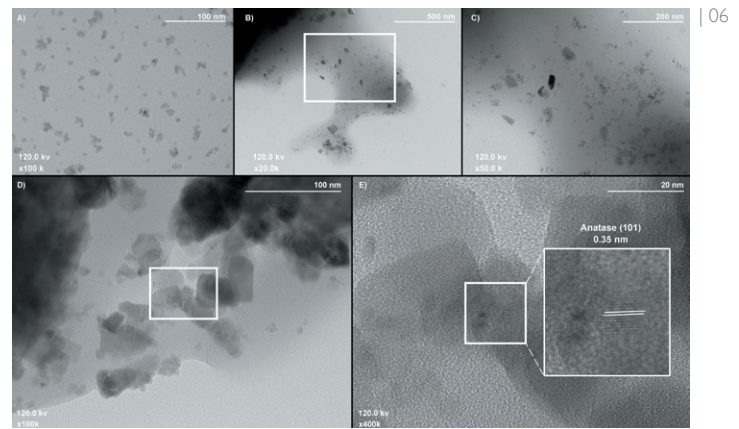
MO2 consisted of a DSC test of Masterbatch and film (Fig. 5). The incorporation of the nanoparticles (ca. 10 [nm] in diameter) into the film does not modify either the transition (T_g) or transformation (T_m) of the polymer. The percentage crystallinity of composites did not show a significant change with nanoparticle incorporation, either during the first heat treatment by extrusion (Masterbatch), or in the second by pressing (film). However, a small increase in crystallinity was observed, which may be explained by a nucleant effect of the nanoparticles (Fonseca et al, 2015).

These observations confirm, in line with the design hypothesis, the potential for mechanical recycling of material using heat, extrusion and pressing treatments, and incorporation of TiO₂ nanoparticles into the process, without significantly altering their thermal properties. This validates the potential use of PETr in the development of new PETr-e-TiO₂ material.

MO3 used TEM analysis to explore the photocatalytic potential of a new material through the incorporation of TiO₂. The nanoparticles were uniformly dispersed throughout the PETr film, with only some agglomerations, proving that homogeneous PETr-e-TiO₂ film can be effectively produced by means of the melting process.

Figure 6 shows TEM images of PETr-e-TiO₂ film prepared by melting. The nanoparticles (8 wt%) were generally well distributed throughout the film (Fig. 6), as shown in images 6B and 6C, although small aggregations can be seen. One limitation revealed by the analysis, visible in images 06B and 06D, is the presence of dark zones. These were due to the fact that the sample was thicker in places than intended, meaning that the beam of electrons was unable to penetrate some zones of the sample. In any case, the outer zones (Fig. 6) show a possible presence of TiO₂ nanoparticles.

In summary, although TEM did not confirm the distribution of the TiO₂ throughout the polymer, our interpretation of the images is



that they are present, along with an anatase structure of TiO₂ nanoparticles (Fig. 6E)

Finally, SEM analysis in MO4 allowed to study the presence and quantity of TiO₂ using a sample taken from the surface, and another within the cross-section of the PETr-e-TiO₂ film. The images exhibit homogeneous surface morphology. The surface image of the composites (Fig. 8B) shows 0.1% titanium dioxide, and the cross-section image (Fig. 7E) shows 0.4% titanium dioxide. This leads to a positive conclusion as to photocatalytic potential resulting from incorporation of TiO₂ nanoparticles.

According to the literature (Loddo et al., 2012) a basic requirement for the removal of contaminating atmospheric gases, such as nitrogen oxides (NO and NO₂), is to ensure the presence of a semiconductor catalyst, such as titanium dioxide (TiO₂), on the capture surface. This promotes oxidation/reduction by ultraviolet light through photocatalysis. If we observe spectra 1, 2 and 3 of the surface sample, we obtain values for the presence of titanium of 4.4%, 11.2% and 17.6%, respectively (Fig. 8). These results are a clear indication of the photocatalytic potential of the new PETr-e-TiO₂ material. Finally, finding TiO₂ nanoparticles on the surface of a 3 mm thick film validates the possibility of developing a semi-finished product.

Conclusions

The use of photocatalysts has been developed primarily based on studies of cement and paint coatings for use in urban infrastructures, such as roadways and footpaths (Liu et al., 2015), and of paints for interior and exterior wall coatings (Maggos et al., 2007). Hence, it possible to identify an emerging market for products used as photocatalytic cladding, such as paints, ceramics and mortars. It is also possible to find some building cladding products made from recycled plastic. However, configuration of new materials based on recy-

pled PET with photocatalytic potential has not been widely considered as part of the development of construction and architectural materials.

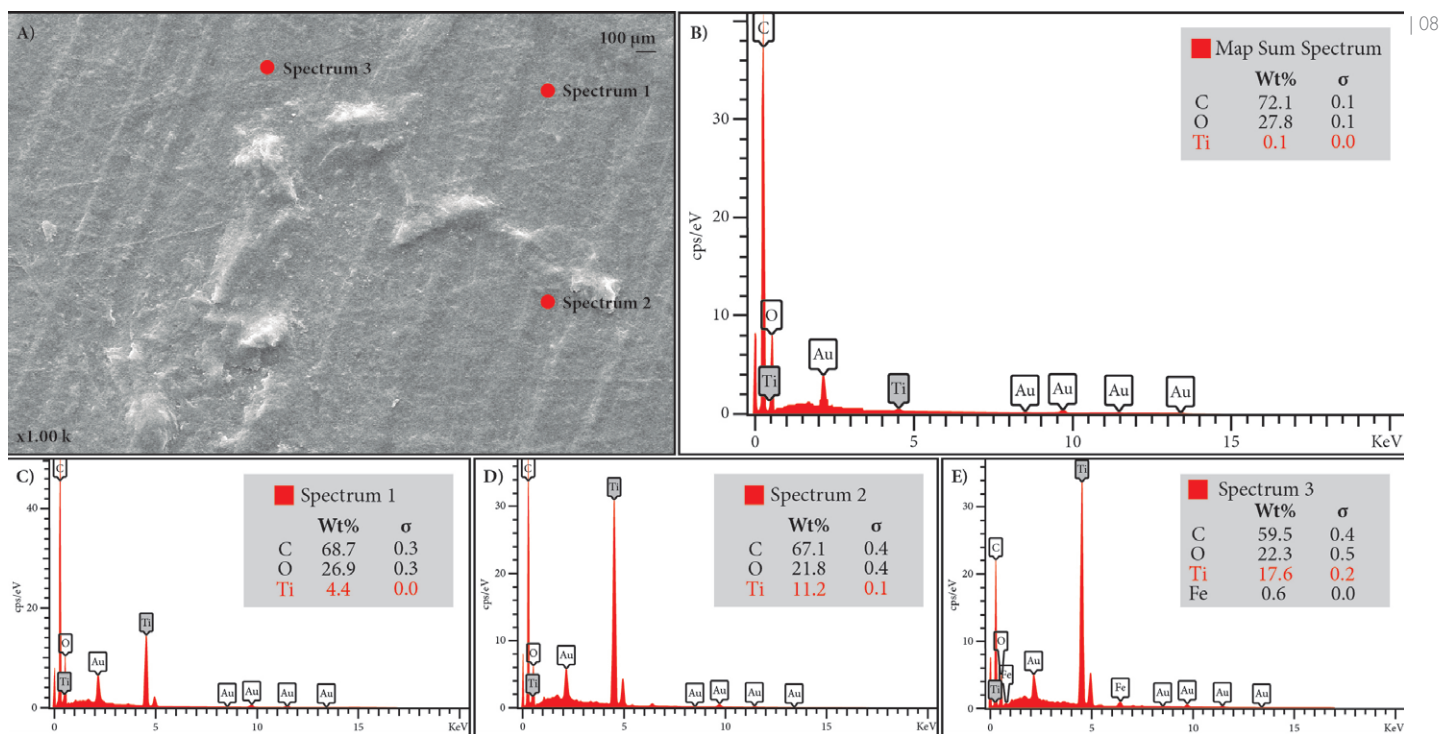
In order to be able to validate this new material as a potential product for the construction market, additional tests must be done, i.e., mechanical, fire and estimation of the energy footprint. As a reference, for the PETr-e-TiO₂ film developed according to the process described in Figure 2, the energy footprint was estimated on 6.67 KWh for each film. Further research should validate this new material as a low energy footprint product.

Concluding, the contribution of the research can be summarised in two important findings. The first is the identification of the presence of TiO₂ nanoparticles (TEM and SEM analysis), particularly on the surface of the films, as this validates the photocatalytic potential. The second finding is the confirmation using DSC analysis of the feasibility of recycling PET waste without altering the thermal properties (T_g and T_m) of the material. An additional outcome of this study is the iterative learning process of *configurations*, involving pressing the three series of film (MO1), which constitutes practical technological laboratory-level knowledge of relevance for future upscaling.

The main concern regarding this progress is the real world effectiveness of the material's photocatalytic potential. However, confirmation of the presence of TiO₂ on the surface of a film that is even 3 mm thick is a positive sign. Future research should seek to assess the material's effectiveness in terms of degradation of different gases, primarily NO_x and SO₂.

Another concern is the tolerance of the film to mechanical forces. This should be validated using tensile, impact and other tests to evaluate the behaviour of the film and, therefore, their potential as a material for tile-type coatings.

Finally, the design of materials with new environmental functions prompts reflection of an iterative relational process of variable adjustment that offers new possible *configurations* for materials design. An acceptance of the challenge to recycle and, as such, to rethink plastic in terms of materials design and new environmental functions – such as the breakdown of contaminating gases – fosters a utopian work structure for design practice. In this framework, managed complexity becomes a platform on which the designer adopts a process of iterative knowledge accumulation while performing an exercise of *configuration* and *materialisation*, both of which are inherent to the exploration of environmental architectural materials.



ACKNOWLEDGMENT

Funded by CONICYT FONDECYT N°11180461 and POSTDOC_DICYT, code 092090CT_AYUDANTE.

REFERENCES

- ASIPLA (2019), *Asipla y la economía circular en Chile*, Asipla.
- Baiani, S. and Altamura, P. (2018), *Waste materials superuse and upcycling in architecture: design and experimentation*, Techne, Journal of Technology for Architecture and Environment, Vol. 16, Firenze University Press, Firenze, pp. 142-151.
- Blaine, R.L. (2002), *Method and apparatus of modulated-temperature thermogravimetry*, US Patent US6336741B1.
- Comisión Europea (2013), *Libro Verde sobre una estrategia europea frente a los residuos de plásticos en el medio ambiente*, Comisión Europea, Bruselas.
- Comisión Europea (2015), *Cerrar el círculo: un plan de acción de la UE para la economía circular*, Comisión Europea, Bruselas.
- Fonseca, C., Ochoa, A., Ulloa, M.T., Alvarez, E., Canales, D., and Zapata, P.A. (2015), *Poly (lactic acid)/TiO₂ nanocomposites as alternative biocidal and anti-fungal materials*. *Materials Science and Engineering*, Vol. 57, pp. 314-320.
- Instituto Nacional de Normalización. INN Chile (1999), *Prevención De incendios en edificios - Parte 1: Determinación del comportamiento de plásticos auto-soportantes a la acción de una llama*, Norma Chilena Oficial NCh 2121/1.Of91
- International standard, (2008) *Plastics - Guidelines for the recovery and recycling of plastics waste*, ISO 15270:2008.
- Loddo, V., Marci, G., Palmisano, G., Yurdakal, S., Brazzoli, M., Garavaglia, L. and Palmisano, L. (2012), "Extruded expanded polystyrene sheets coated by TiO₂ as new photocatalytic materials for foodstuffs packaging". *Applied Surface Science*. Vol. 261, pp. 783-788.
- Liu, W., Wang, S.Y., Zhang, J. and Fan, J. (2015), "Photocatalytic degradation of vehicle exhausts on asphalt pavement by TiO₂/rubber composite structure", *Construction and Building Materials*, Vol. 81, pp. 224-232.
- Maggos Th., Bartzis J.G., Liakou M. and Gobin C. (2007), "Photocatalytic degradation of NOx gases using TiO₂-containing paint: A real scale study", *Journal of Hazardous Materials*, Vol. 146, pp. 668-673.
- Manzini, E., (1992), *Artefactos. Hacia una nueva ecología del ambiente artificial*, Celeste Ediciones.
- Instituto Nacional de Normalización INN Chile (1999), *Construcción - Baldosas Plásticas - Métodos de Ensayo*, Norma Chilena Oficial NCh 873.Of1999.
- Rose, C. and Stegemann, J. (2018), *From Waste Management to Component Management in the Construction Industry*, *Sustainability*, Vol.10 (1), pp. 2-21.